Article

Study on the Best Water Cushion Depth of Stilling Basin with Shallow-Water Cushion at Different Froude Numbers

Qiulin Li [1], Lianxia Li [1,*], Huasheng Liao [2], Jingjing Wei [1], Shengyin Jiang [3] and Faxing Zhang [1]

1 State Key Laboratory of Hydraulics and Mountain River Development and Protection, College of Water Resource and Hydropower, Sichuan University, Chengdu, Sichuan, 610065, China; 18523904606@163.com (Q.L.); 1679535001@qq.com (J.W.); faxingzhang@scu.edu.cn (F.Z.)

2 Michigan State University, East Lansing, USA; liao@egr.msu.edu

3 Chengdu Municipal Engineering and Research Design Institute, Chengdu, Sichuan, 610065, China; scujsy@163.com

* Correspondence: lianxiali@scu.edu.cn; Tel.:+86 13308021514

Abstract: The water cushion depth of stilling basin with shallow-water cushion is a key factor that affects the flow regime of hydraulic jump in the basin. However, the specific depth at which the water cushion is considered as "shallow" has not be stated clearly for now, and only conceptual description is provided. This paper attempts to specify the best water cushion depth based on the flow regime of hydraulic jump and underflow speed; namely, in case of critical hydraulic jump in the basin, the best water cushion depth is located where the minimum distance to the bottom plate of the stilling basin is 1/5~1/4 of the water cushion depth. The theoretical analysis indicates, at different inclinations of discharge chute (θ) and depth ratios of inlet (m), instead of monotonic change, the Froude number (Fr) at inlet of the stilling basin with shallow-water cushion firstly reduces and then increases as the flow velocity at discharge chute inlet (V) increases; the parameters of inflection point (critical flow velocity and critical Fr) increase as the inclinations of discharge chute (θ) and depth ratios of inlet (m) increase. Such regularity is the theoretical basis for selecting representative study cases. The reliability of the large eddy simulation calculation results are verified by a model test; in the paper, 30 cases including five different Froude numbers and six shallow-water cushion depths are selected, for calculating the hydraulic factors such as flow profile, flow regime and flow velocity in the stilling basin with shallow-water cushion; and the varying pattern between the best depth of stilling basin with shallow-water cushion (depth-to-length ratio) and the inflow Froude number is obtained which indicates that the best depth of stilling basin with shallow-water cushion varies little as the change of the Froude number before reaching the critical Froude number; however, the best depth-to-length ratio of stilling basin with shallow-water cushion increases as the Froude number increases after the critical Froude number is reached. The study results in this paper are of reference significance to design and calculation of the stilling basin with shallow-water cushion.

Keywords: energy dissipation; hydraulic jump; Froude number; stilling basin with shallow-water cushion; large eddy simulation; hydraulic characteristics

0 Introduction

At present, the energy dissipation by hydraulic jump is used for downstream in many hydraulic projects [1], of which stilling basin plays an important role in energy dissipation. However, the traditional stilling basin [2-4] has disadvantages such as high underflow speed near the bottom, apparent damages by erosion and cavitation [5] as well as insufficient energy dissipation rate. Many researchers have made studies on such problems. Early in 2006, Li Tianxiang[6] et al. of Sichuan

 doi:10.20944/preprints201710.0147.v1

University introduced the concept of stilling basin with shallow-water cushion; namely, a shallow-water cushion is added for the ordinary stilling basin. In the structure of the new type stilling basin, the water cushion formed at the basin bottom can be used as the “flexible bottom plate”, which applies a flexible counterforce to the water stream in the steep slope section and “absorbs” part impact force of the water stream, so as to realize the purpose of "conquering the unyielding with the yielding". After that, Ru Yongshen and Su Peilan[7,8] made a detailed study on the hydraulic characteristics of the stilling basin with shallow-water cushion. Liu Da and Liao Huasheng[9] made a study on large eddy simulation of the stilling basin with shallow-water cushion. Li Lianxia and Liu Da[10-12] et al. made a series of studies on the impact caused by inlet type, inflow angle and low Froude number of the stilling basin with shallow-water cushion on its hydraulic characteristics. Liu Da, Jiang Shengyin and Li Lianxia[13,14] also proposed the concept of stilling basin with double shallow-water cushions. It has the advantages same to those of the stilling basin with shallow-water cushion, as well as better hydraulic characteristics, lower underflow speed and better distribution of dynamic pressures of bottom plate of the stilling basin. Wan Jiwei et al. [15] proposed the concept of stilling basin with small bucket angle, drop sill and shallow-water cushion. Compared with the common stilling basin, it is of a simpler shape, and can effectively solve the problems such as weak adaptability and inflexible operation way in the similar gate dam projects with high unit discharge, low Froude number and great water level amplitude between upstream and downstream. The stilling basin with drop sill is similar to the stilling basin with shallow-water cushion not only in type, but also in study means and method. Sun Shuangke[16] et al. made a study on the hydraulic characteristics of the stilling basin with drop sill. Yang Yongsen [17] made a study on the mechanism of energy dissipation of abrupt drop type stilling basin at low Froude numbers. The stilling basin with drop sill [18-24] is very similar to the stilling basin with shallow-water cushion. However, the former one is focused on the connection type of drop sill at the stilling basin inlet, while the latter one is focused on the energy dissipation mechanism of the stilling basin and the effect of the shallow-water cushion.

The water cushion depth of the stilling basin with shallow-water cushion is of a critical importance to the energy dissipation effect of the stilling basin. However, no systematic study has been made on that influence factor for now. Besides, whether the water cushion is considered as deep or shallow has not been defined clearly since the concept of stilling basin with shallow-water cushion was proposed. This paper proposes the definition of the best shallow-water cushion depth on the basis of existing study results on the stilling basin with shallow-water cushion; namely, the water cushion depth at which the critical hydraulic jump occurs in the basin and the distance from the main stream to the bottom plate is 1/5~1/4 of the water cushion depth. If the water cushion depth is higher than the best depth, it is not necessary; if the water cushion depth whereas is lower than the best depth, the buffer action of the water cushion can not be given full play to. Based on that standard and the theoretical analysis, after verifying the reliability of numerical model, the method of large eddy simulation is used for a comprehensive study on the pattern of affecting the hydraulic characteristics of stilling basin by the shallow-water cushion depth. This study is not about to select a specific inflow Froude number, but to study the shallow-water cushion depths required at different Froude numbers, so as to obtain the best shallow-water cushion depth (represented by dimensionless depth-to-length ratio, which is convenient for application) corresponding to the specified Froude number based on the hydraulic parameters such as flow regime and flow field distribution in the stilling basin.

1 Methodology

In this study, the feasibility and accuracy of hydraulic characteristics of the stilling basin with shallow-water cushion as simulated in large eddy simulation are verified based on the results of physical test model, and then the theoretical analysis is conducted to obtain the varying pattern of Froude numbers and inlet conditions at the stilling basin inlet, so as to select 30 operating conditions, including five Froude numbers and six shallow-water cushion depths, for calculation and comparison.

Preprints (www.preprints.org) | NOT PEER-REVIEWED | Posted: 23 October 2017 doi:10.20944/preprints201710.0147.v1

1.1 Test model

The test device is composed of several sections including the inflow discharge chute section, baffle as well as the section of stilling basin with shallow-water cushion and tail water section (as shown in Fig. 1). The discharge chute section and all downstream parts are with rectangular cross section, with the width of 30cm. The radial gate is used upstream of the model. The discharge volume is controlled by different water levels in the water tank. The gate opening is 10cm in all occasions. The discharge chute section is with the length of 363cm. The slope used in this study is fixed to 17°. The stilling basin section is with the length of 120cm. The tail water section is with the length of 300cm. At downstream, the water level will not be controlled, free discharge is applied. The flow profile is measured by the grid method. Criss-cross coordinate grid (Fig. 2) is provided on the side wall. The flow velocity is measured by the LS300-A type current meter.

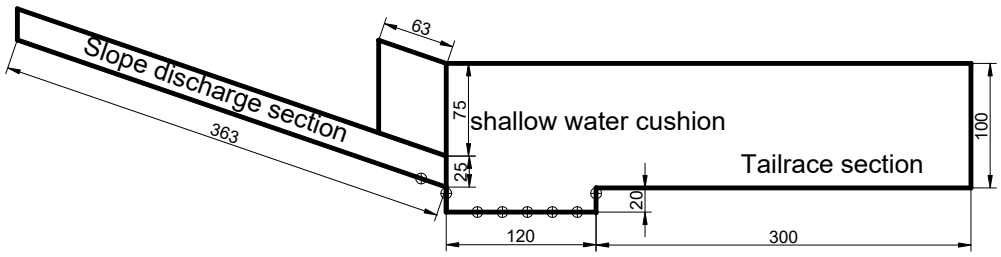

Fig. 1 Layout drawing for model test (in cm)

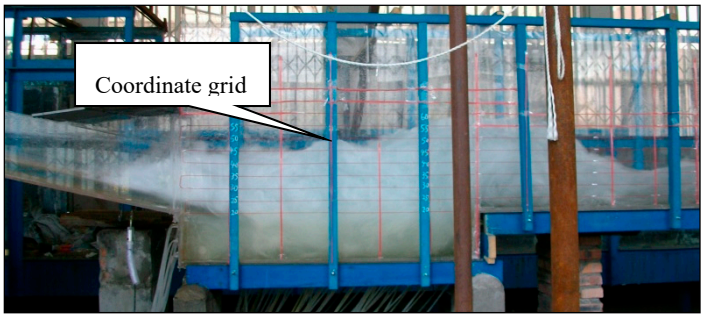

Fig. 2 Water flow regime of section of stilling basin with shallow-water cushion indicated in model test

1.2 Theoretical method

The Froude number at the stilling basin inlet is affected by many factors. In order to obtain the varying pattern related to the Froude number and select representative Froude numbers for calculation, theoretical analysis method is used in this study to study the Froude numbers at the stilling basin inlet.

Take the inlet and terminal of the chute section as the control sections 1-1 and 2-2 respectively, and take the elevation at the terminal of the discharge chute as the reference elevation, so as to establish the energy equation and continuity equation. For simplification, take the speed at the inlet as the speed in the frictional head loss item, and take the hydraulic radius at the inlet; the energy equation is expressed as the Equation (1),

$$Z_1 + \frac{\alpha_1 V_1^2}{2g} = Z_2 + \frac{\alpha_2 V_2^2}{2g} + \xi \frac{V_1^2}{2g} + \lambda \frac{L}{4R_1} \frac{V_1^2}{2g} \quad (1)$$

And the continuity equation is expressed as the Equation (2),

$$V_1 h_1 B_1 = B_2 h_2 B_2 \quad (2)$$

Preprints (www.preprints.org) | NOT PEER-REVIEWED | Posted: 23 October 2017 doi:10.20944/preprints201710.0147.v1

where, the subscripts 1 and represents the inlet location of the discharge chute and the terminal location of the discharge chute respectively; Z represents the height from the control section to the reference elevation; α represents the kinetic energy correction factor; V represents the flow velocity; ξ represents the local head loss coefficient of the inlet; λ represents the frictional head loss coefficient; R represents the hydraulic radius; h represents the depth of water at the inlet of discharge chute; B represents the width of the discharge chute; the Froude number at the terminal of the discharge chute can be obtained by the simultaneous equations (1) and (2), which is also the Froude number at the stilling basin inlet (according to the flow regime, the above two Froude numbers are with little difference; for simplification, they are not distinguished).

$$Fr=\frac{\left(\frac{2gm\sin\theta+\left(\frac{\alpha_1}{h}-\frac{\xi}{h}-\frac{\lambda}{4R}m\right)V^2}{\alpha_2}\right)^{\frac{3}{4}}}{(gV)^{\frac{1}{2}}h^{-\frac{1}{4}}} \tag{3}$$

Where, m=L/h, L represents the length of the discharge chute, h represents the depth of water at the discharge chute inlet, and θ represents the inclination of the discharge chute.

The Equation (3) can be simplified to $Fr=f(V,m,\theta)$; where, V is an independent variable, m and θ are parameters; in the test, B=0.3m, h=0.1m, α_1=1.05, α_2=1.1, ξ=0.5, $R_1=\frac{A_1}{\chi_1}$=0.06, n=0.01, $C=\frac{1}{n}R^{1/6}$, $\lambda=\frac{8g}{C^2}$=0.020047。

In order to select representative operating conditions to be used in the test, the following method is used to determine the Froude number at the stilling basin inlet:

Step 1: according to the model dimension, turn the Equation (3) into the Equation (4) after confirming m = 36.3,

$$Fr=\frac{\left(647.46Sin\theta+2.245V^2\right)^{3/4}}{5.67V^{0.5}} \tag{4}$$

The relation between flow velocity at the discharge chute inlet and the Froude number at stilling basin inlet at different θ (the inclination of discharge chute) can be obtained based on the Equation (4), as shown in Fig. 3.

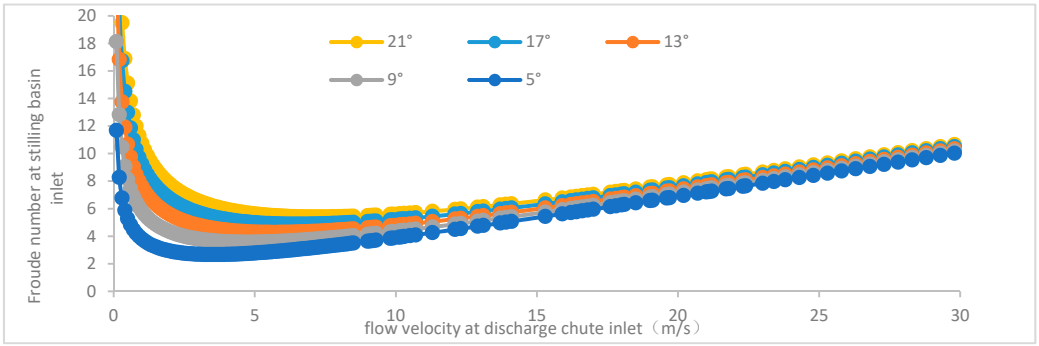

Fig. 3 Relation between flow velocity at discharge chute inlet and Froude number at stilling basin inlet at different inclinations

As shown in the figure, at the same inclination, the Froude number reduces firstly and then increases as the flow velocity varies, during which an inflection point will be inevitable; the inflection point may be located at different places at different inclinations. Further, to obtain the varying pattern

Preprints (www.preprints.org) | NOT PEER-REVIEWED | Posted: 23 October 2017 doi:10.20944/preprints201710.0147.v1

between the position of the inflection point and the inclination of the discharge chute, calculate the derivative of the flow velocity (V) in the Equation (4); taking that derivative as 0, the flow velocity relation corresponding to the inflection point in Fig. (4) at different inclinations can be obtained by (5)

$$V^2 = 144.171 Sin\theta \tag{5}$$

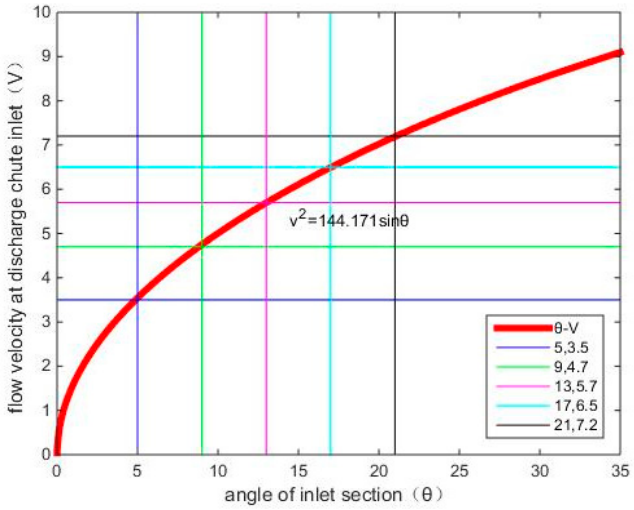

Fig. 4 Flow velocity of inflection points related to different inclinations

As shown in Fig. 4, the velocity corresponding to the inflection point increases as the inclination increases; the Froude number of the inflection point related to each inclination in Fig 3 is 5.3, 4.8, 4.2, 3.5 and 2.6 respectively.

Step 2: select the inclination of the discharge chute, and then obtain the relation between the flow velocity (V) at the discharge chute inlet and the Froude number (Fr) at the stilling basin inlet under different parameters. In this study, the inclination (θ) is 17°, the Equation (3) is turned into the Equation (6), and the corresponding function image is shown in Fig. 5.

$$Fr = \frac{\left(5.22m + \left(5 - 0.076m\right)V^2\right)^{3/4}}{5.67V^{0.5}} \tag{6}$$

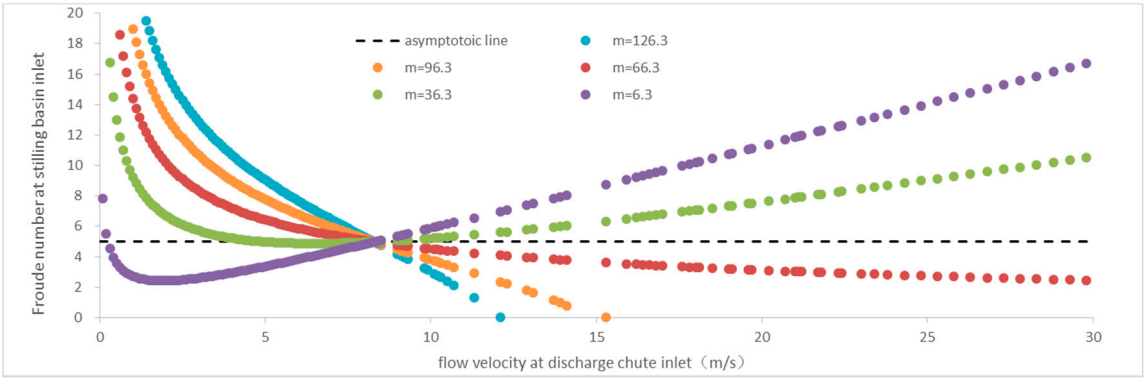

Fig. 5 Relation between flow velocity and Froude number at different ratios of discharge chute length and inlet height

As shown in Fig. (5), the variation trend between Froude number and flow velocity is different at different ratios; when m is relatively low, the variation trend is increase after reduction; when m is relatively high, and the flow velocity and Froude number are in monotone decreasing function. To obtain the varying pattern of the inflection point, calculate the derivative of the flow velocity (V) in

Preprints (www.preprints.org) | NOT PEER-REVIEWED | Posted: 23 October 2017 doi:10.20944/preprints201710.0147.v1

the Equation (6), and taking the derivative as 0. The flow velocity of inflection point at different ratios (m) is shown in the Equation (7), and the function image is shown in Fig. 6.

$$V^2 = \frac{2.868m}{5.5-0.084m} \tag{7}$$

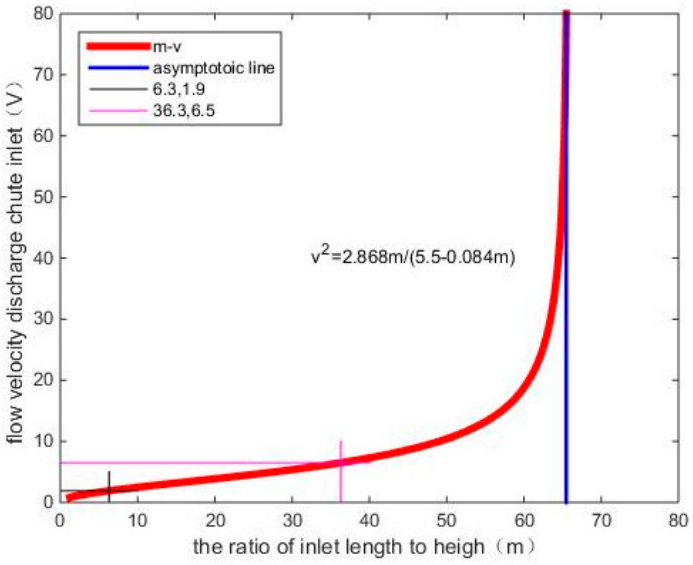

Fig. 6 Relation between flow velocity (V) at discharge chute and m

As shown in Fig. 5, the velocity corresponding to the inflection point increases as the ratio increases; however, the ratio is with a certain limit, and the curve is infinitely close to: m=65.476 (see Fig. 6); therefore, if m is less than 65.476, the relation between Fr and V is not in a monotonic curve, and there is an inflection point; if m equals to 36.3 or 6.3, the Froude number at the corresponding inflection point is 4.8 and 2.4 respectively. If m is greater than 65.476, the Equation (6) is a monotone decreasing function, and the three curves (m=66.3, 96.3 and 126.3 respectively) in Fig. 5 intersect with the x axis, because simplification is assumed when deriving the Equation (6) by the energy equation of the Equation (1). Namely, parameters such as the velocity and hydraulic radius at the discharge chute inlet are used when calculating the frictional head loss. Actually, such parameters varies along the way, the error will be low if the length of the discharge chute is small (i.e., m is relatively low); if m is relatively high, such assumption is not applicable. In this study, the discharge chute is short (m=36.3), thus the error caused by such simplification is small.

1.3 Mathematical model

The mathematical model of large eddy simulation is used in the calculation, which is introduced below.

1) Control equation

In large eddy simulation [25-28] (LES), the large-scale eddy is simulated directly by solving the momentum equation, and the small-scale eddy is expressed in the sub-grid scale model. The control equation is:

$$\frac{\partial \rho}{\partial t} + \frac{\partial (\rho \overline{u_i})}{\partial x_i} = 0 \tag{8}$$

Preprints (www.preprints.org) | NOT PEER-REVIEWED | Posted: 23 October 2017 doi:10.20944/preprints201710.0147.v1

$$\frac{\partial(\rho\overline{u_i})}{\partial t}+\frac{\partial(\rho\overline{u_i}\overline{u_j})}{\partial x_j}=-\frac{\partial\overline{p}}{\partial x_i}+\frac{\partial}{\partial x_j}\left(\mu\frac{\partial\overline{u_i}}{\partial x_j}\right)-\frac{\partial\tau_{ij}^{sgs}}{\partial x_j}+\rho g_i \tag{9}$$

Where, the value with "-" represents the large-scale value obtained after filtering,; ρ represents the density; U represents the velocity; t represents the time,; p represents the pressure; g represents the acceleration of gravity; x represents the coordinate; i, j represents the coordinate orientation; and τ_{ij}^{sgs} represents the sub-grid stress, which indicates the impact caused by small-eddy movement on the large-eddy movement. Generally, the sub-grid stress is calculated by the eddy viscidity model:

$$\tau_{ij}^{sgs}-\frac{1}{3}\tau_{kk}^{sgs}\delta_{ij}=-2\mu_{sgs}\overline{S_{ij}} \tag{10}$$

Where, μ_{sgs} represents the sub-grid turbulent viscosity coefficient, $\delta_{ij}=\begin{cases}1, & i=j\\ 0, & i\neq j\end{cases}$; $\overline{S_{ij}}$ represents the strain rate tensor under the scale to be solved, which is defined as;

$$\overline{S_{ij}}=\frac{1}{2}\left(\frac{\partial\overline{u_i}}{\partial x_j}+\frac{\partial\overline{u_j}}{\partial x_i}\right) \tag{11}$$

The Smagorinsky-Lilly model is used to calculate the sub-grid turbulent viscosity coefficient: $\mu_{sgs}=\rho L_s^2\sqrt{2\overline{S_{ij}}\cdot\overline{S_{ij}}}$, $L_s=\min\left(\kappa d, C_s V^{1/3}\right)$; where, L_s represents the mixed length of the sub-grid scale; κ represents the Karman constant; d represents the distance to the nearest wall face; V represents the volume of computing control body; and C_s represents the Smagorinsky constant, which is 0.1 in this study.

2) Discrete and solving

In this test, the finite volume method is used to discrete of the control equation, and second-order implicit scheme is used in the discretization of time item, and the PISO algorithm is used to solve and control the coupling of velocity and pressure in the equation. The VOF method is used to track and simulate the free surface and two-phase flow of air and water. The free water surface is established by the geometrical reconstruction scheme.

3) Computational domain and boundary conditions

(1) Computational domain

The computational domain is shown in Fig. 7. The water intake is with the opening of 10cm. A baffle is provided at both sides of the upstream intake section of the stilling basin respectively, so as to avoid overflow during the intermediate iteration process.

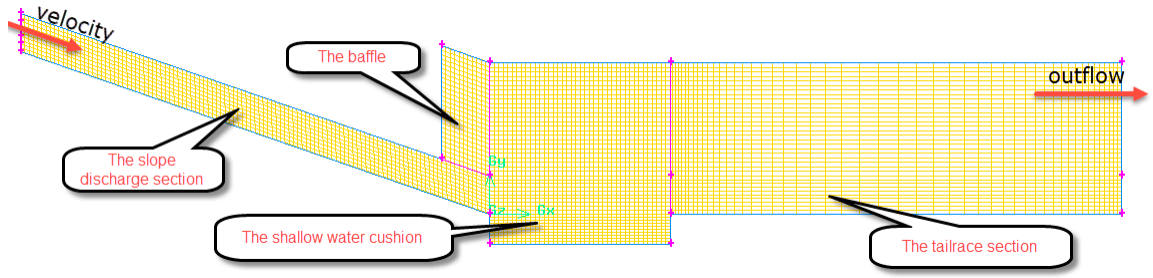

Fig. 7 Schematic diagram for computational domain of mathematical model

Preprints (www.preprints.org) | NOT PEER-REVIEWED | Posted: 23 October 2017 doi:10.20944/preprints201710.0147.v1

The grids in the stilling basin and tail water section are transited from coarse to fine from top to bottom which size is 2cm~3cm. The longer edge of the grid is with the dimension of 3cm. The model is with 57,200 grids in total.

(2) Boundary conditions

The boundary condition of the inlet of the chute is set as velocity inlet condition which can be determined according to the relationship between inlet velocity and inlet Froude number of stilling basin discussed in section 1.2. Free discharge[29] is applied at the outlet boundary. The viscous sublayer of the near wall is treated by the wall function method. Non-slip condition is applied on the fixed wall.

4. Verification of mathematical model

The test results are selected to compare with the calculation results of the large eddy simulation. The flow velocity at the discharge chute inlet is 0.5m/s, 1m/s and 6.5m/s respectively. The depth of the stilling basin with shallow-water cushion is 20cm, 15cm and 25cm respectively.

(1) Flow regime comparison

Fig. 8 shows water flow regimes in the stilling basin under the three conditions. It is observed that, both the test and computation show good hydraulic jump in the stilling basin, with intense turbulence on water surface.

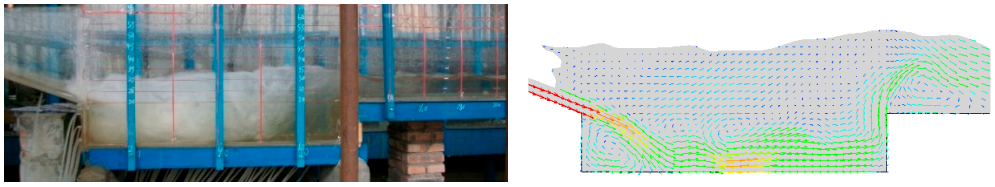

(a) The flow velocity at the chute inlet is 0.5m/s, and the basin depth is 20cm.

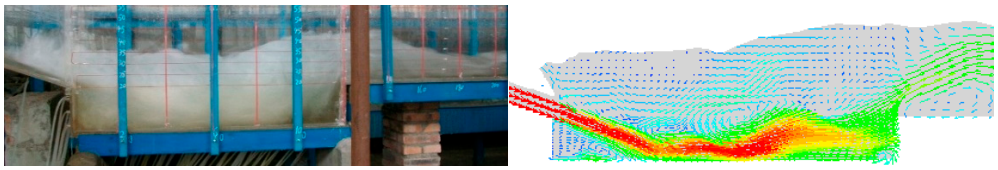

(b) The flow velocity at the chute inlet is 1m/s, and the basin depth is 15cm.

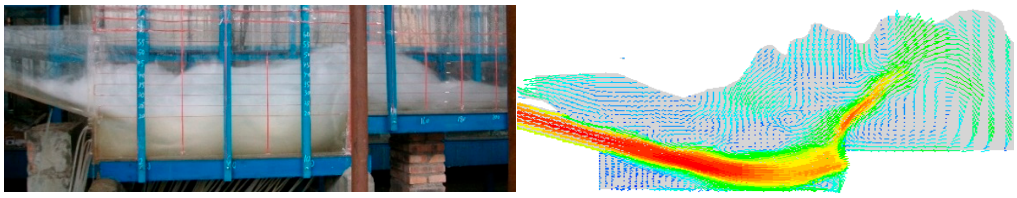

(c) The flow velocity at the chute inlet is 6.5m/s, and the basin depth is 25cm.

Fig. 8 Schematic diagram for flow regimes under three conditions

(2) Comparison of flow profile

The comparison of flow profiles between test results and calculated results show good agreement with each other (Fig. 9) which verifies the reliability of large eddy simulation again.

Preprints (www.preprints.org) | NOT PEER-REVIEWED | Posted: 23 October 2017 doi:10.20944/preprints201710.0147.v1

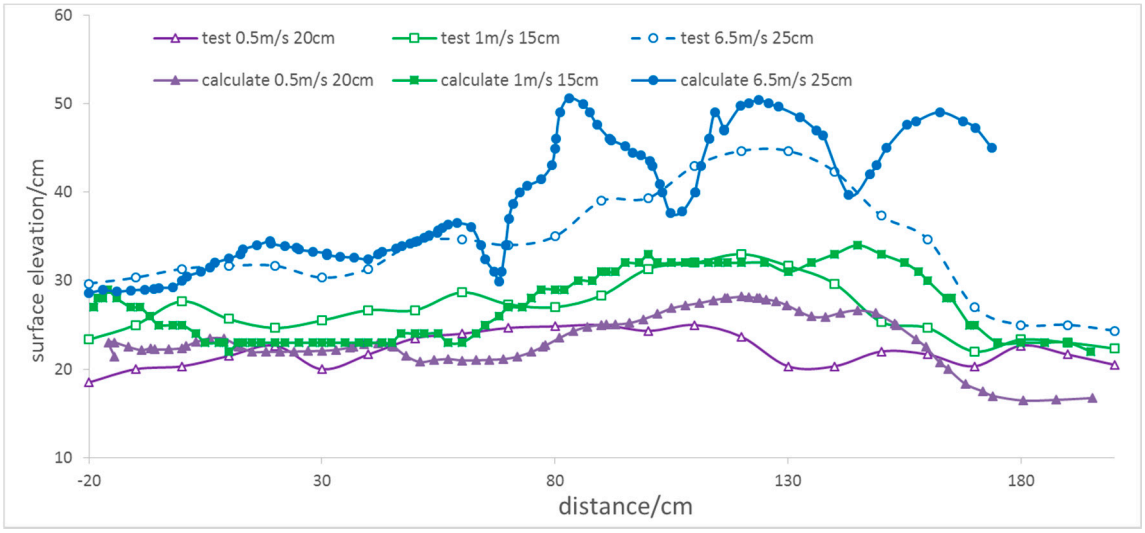

Fig. 9 Comparison of flow profile

2 Results and discussion

According to the varying pattern among the Froude number (Fr) at the inlet of the stilling basin with shallow-water cushion, inlet flow velocity (V) and model dimensions (m and θ) as obtained by the aforesaid analysis as well as the dimensions of physical model (m=36.3, θ=17°), five values of the flow velocity at the discharge chute inlet are determined (V=0.5m/s, 1m/s, 2m/s, 6.5m/s and 8m/s), so that the different Froude numbers at the stilling basin inlet are obtained (Fr=13.03, 9.41, 6.71, 4.89, 5.17). When Fr equals to 4.89, it corresponds to the inflection point (i.e., the critical Froude number) on the curve (Figs 3 and 5), and the corresponding critical flow velocity (V) at the discharge chute inlet is 6.5m/s. Six different basin depths are used, including 0cm, 5cm, 10cm, 15cm, 20cm and 25cm, and the length is fixed to 120cm, so that six different depth-to-length ratios of the shallow-water cushion are obtained: 0, 0.042, 0.083, 0.125, 0.167, 0.208. The 30 cases for calculation include five typical Froude numbers and six different depths of shallow-water cushion.

According to five different inflow Froude numbers, systematic study was conducted on the varying pattern of hydraulic characteristics such as flow profile, flow velocity and flow regime in the stilling basin with different depths of the shallow-water cushion, so as to determine the best depth of the shallow-water cushion. Namely, at the best depth, the main stream is located at the position about 1/3 depth of the shallow-water cushion and with the distance about 1/5 depth to the cushion bottom, and the critical hydraulic jump occurs in the stilling basin.

2.1 Fr=13.03 (V=0.5m/s)

(1) Flow regime and flow profile

The occurrence conditions of hydraulic jump in the stilling basin are different at different depths according to the water flow regimes in the stilling basin at six depths (d) of shallow-water cushion which are presented in Fig. 10. In case that the water cushion depth is 0cm, there is no hydraulic jump along downstream the discharge chute. In case that the water cushion depth is 5cm, the water surface in the stilling basin is flat, and no hydraulic jump occurs. In case that the water cushion depth is 10cm, there is fluctuation in water in the stilling basin, and hydraulic jump in far-forth driving form occurs. In case that the water cushion depth is 15cm, there is an intense fluctuation of water body in the stilling basin, and critical hydraulic jump occurs. When the water cushion depth is 20cm or 25cm, the stilling basin is occupied by a large water body, and submerged type hydraulic jump occurs. Therefore, in terms of flow regime, relatively perfect hydraulic jump occurs in the stilling basin when the shallow-water cushion depth is 15cm (depth-to-length ratio: 0.125).

Preprints (www.preprints.org) | NOT PEER-REVIEWED | Posted: 23 October 2017 doi:10.20944/preprints201710.0147.v1

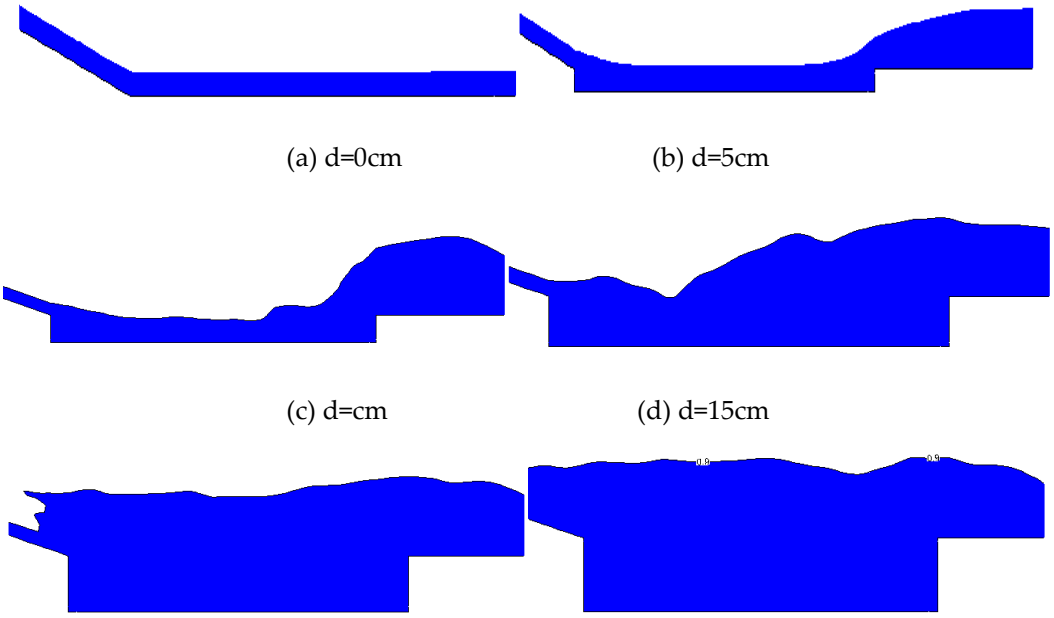

(a) d=0cm (b) d=5cm

(c) d=cm (d) d=15cm

(e) d=20cm (f) d=25cm

Fig. 10 Schematic diagram for flow regimes under six conditions

From comparison of profiles of free surface in the stilling basin at six depths of shallow-water cushion (Fig. 11), the same observation can be seen that the flow profiles under different conditions vary greatly, and relatively perfect flow profile is obtained when the water cushion depth is 15m.

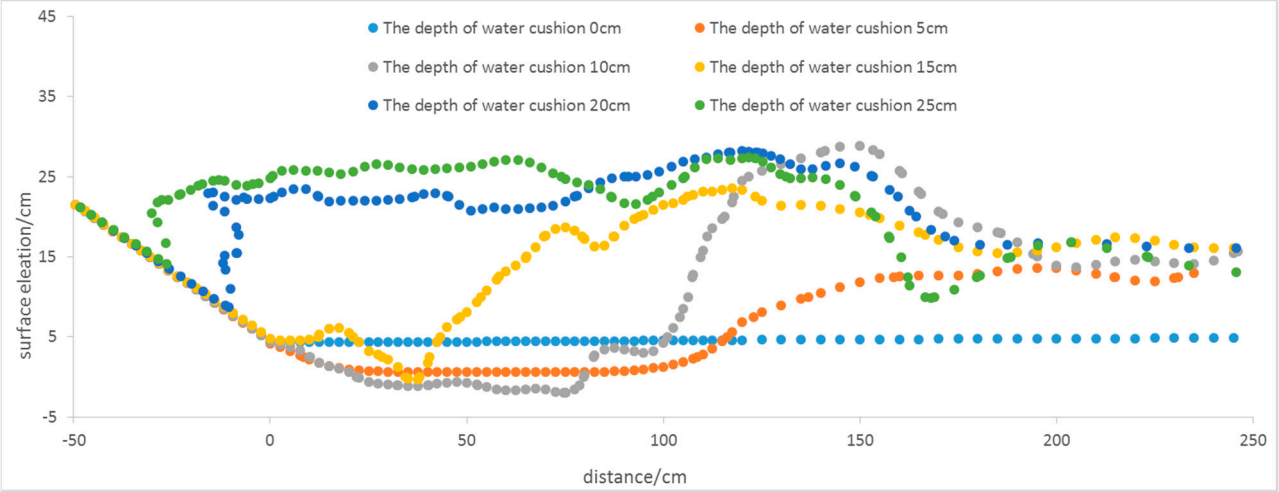

Fig. 11 Comparison of flow profiles at different water cushion depths (Fr=13.03)

(2) Flow field structure

Velocity fields of local flow in the six stilling basins are presented in Fig.12. It shows that under different conditions, the water flow is different at the inlet and the stilling basin section, and the velocity varies differently in the vertical direction, and the quantity and intensity of the vortex generated in the water flow are different. When water flows to the tail ridge of the stilling basin, the reduction of flow velocity and vortex range change are with distinct difference.

Preprints (www.preprints.org) | NOT PEER-REVIEWED | Posted: 23 October 2017 doi:10.20944/preprints201710.0147.v1

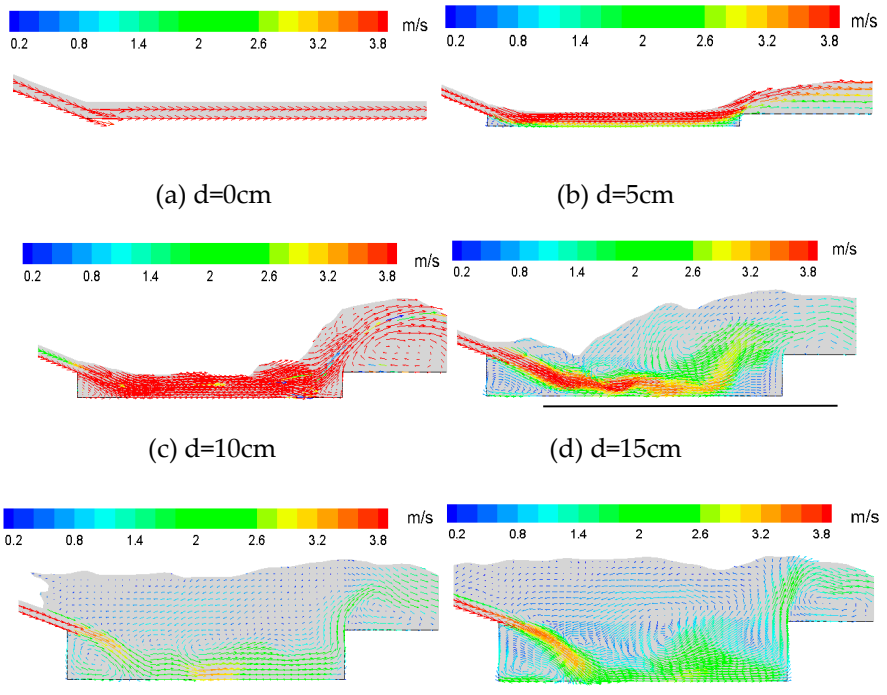

(a) d=0cm (b) d=5cm

(c) d=10cm (d) d=15cm

(e) d=20cm (f) d=25cm

Fig. 12 Velocity vector of local flow in stilling basin

In case of no shallow-water cushion (0cm), the flow velocity downstream the chute is not reduced obviously, and there is no vortex in the water flow, and the main stream impacts the floor. If the depth of the shallow-water cushion is 5cm, water flow turns at the inlet and outlet of the stilling basin and a partial vortex area is formed, and the flow velocity in the stilling basin is high, and the main stream touches the bottom. If the basin depth is 10cm, at the front end of the stilling basin, the flow velocity is high, and there are only a few vortexes; there are more vortexes occurring at the terminal of the basin; meanwhile the flow velocity is still high, and the main stream touches the bottom. If the basin depth is 15cm, the flow velocity in the front end of the stilling basin is higher than that in the tail end, and the water body of energy dissipation is larger compared with the aforesaid three conditions, and there is a water layer of 1/5 basin depth from the main stream to the bottom (The black line in Fig. 12(d) is with the distance of 1/5 basin depth to the bottom plate.), and relative shallow-water cushion is obtained. If the basin depth is increased to 20cm or 25cm, the water body of dissipation gets larger with wider range vortex, and the flow velocity has been reduced greatly in the front end of the stilling basin, and there is a deep water layer below the main stream, and an obvious submerged hydraulic jump has been occurred.

Based on the flow regime and flow field distribution of the hydraulic jump, when Froude number equals to 13.03, the best depth of shallow-water cushion is 15cm and the corresponding related depth-to-length ratio is 0.125.

2.2 Fr=9.41 (V=1m/s)

(1) Flow regime and flow profile

The occurrence conditions of hydraulic jump in the stilling basin are different at different depths according to the water flow regimes in the stilling basin at six depths (d) of shallow-water cushion which are presented in Fig. 13. In case that the water cushion depth is 0cm (there is no shallow-water cushion), 5cm or 10cm, the water flow regime is similar along downstream the discharge chute and in the shallow-water cushion, and it varies as follows: there is no hydraulic jump, the flow regime bends, and hydraulic jump in far-forth driving form occurs. In case that the basin depth is 15cm, there

Preprints (www.preprints.org) | NOT PEER-REVIEWED | Posted: 23 October 2017 doi:10.20944/preprints201710.0147.v1

is intense fluctuation in water in the basin, critical hydraulic jump occurs, and the water flow regime is relatively perfect. In case that the basin depth is 20cm or 25cm, the stilling basin is occupied by a large water body, and the submerged type hydraulic jump occurs. Therefore, in terms of flow regime, relatively perfect hydraulic jump occurs in the stilling basin when the shallow-water cushion depth is 15cm (depth-to-length ratio: 0.125).

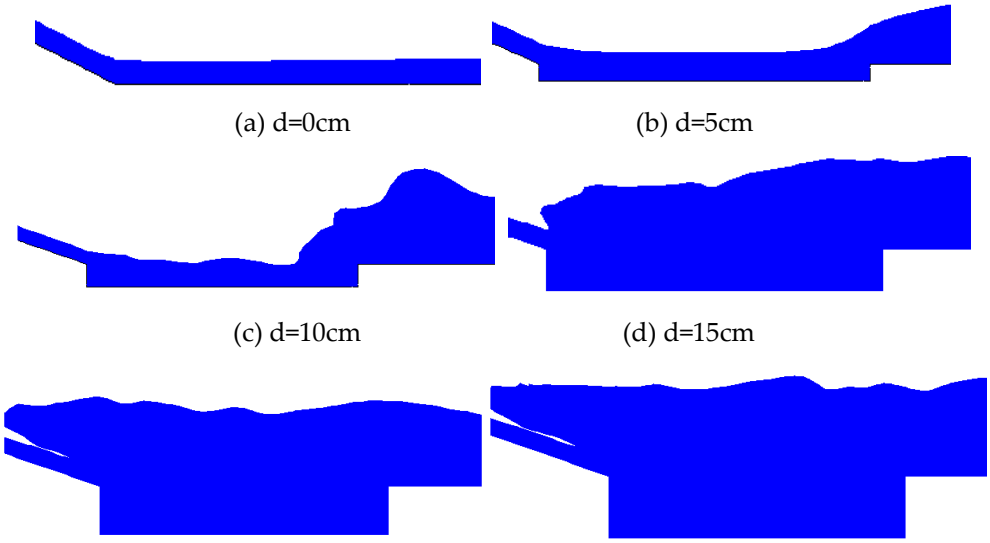

(a) d=0cm (b) d=5cm

(c) d=10cm (d) d=15cm

(e) d=20cm (f) d=25cm

Fig. 13 Schematic diagram for flow regimes under six conditions

From comparison of profiles of free surface in the stilling basin at six depths of shallow-water cushion (Fig. 14), the same observation can be seen that the flow profiles under different conditions vary greatly, and relatively perfect flow profile is obtained when the shallow-water cushion depth is 15cm.

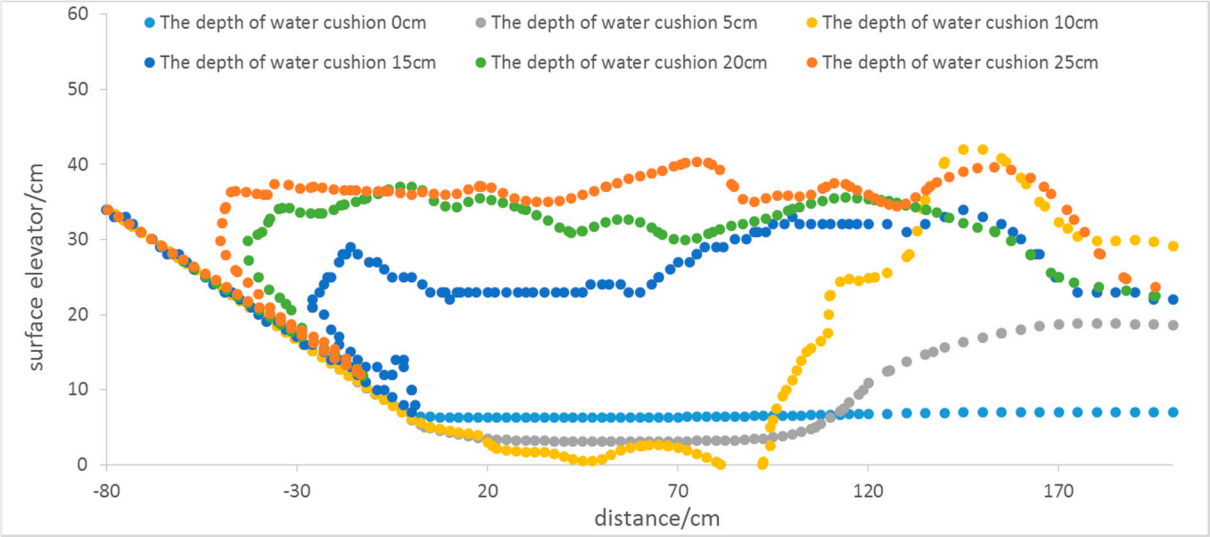

Fig. 14 Comparison of flow profiles at different water cushion depths (Fr=9.41)

(2) Flow field structure

Velocity fields of local flow in the six stilling basins are presented in Fig.15. It shows that under different conditions, the water flow is different at the inlet and the stilling basin section, and the

Preprints (www.preprints.org) | NOT PEER-REVIEWED | Posted: 23 October 2017 doi:10.20944/preprints201710.0147.v1

velocity varies differently in the vertical direction, and the quantity and intensity of the vortex generated in the water flow are different.

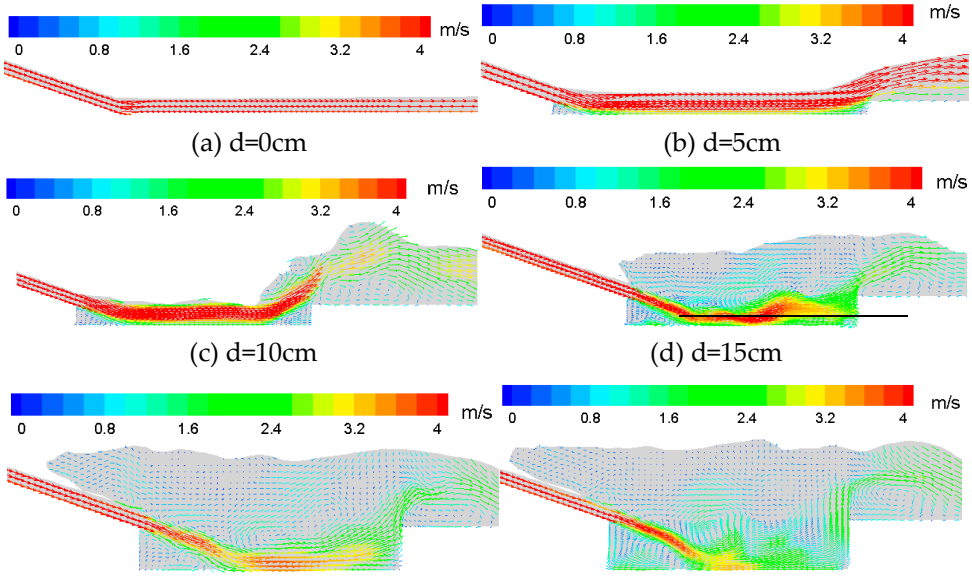

Fig. 15 Velocity vector of local flow in stilling basin

Compared with the six shallow-water cushion depth conditions when the Froude number is 13.03 as shown in Fig. 12, the flow velocity vector charts corresponding to six depths shown in Fig. 15 are similar. In case of no shallow-water cushion (0cm), the flow velocity downstream the chute is not reduced obviously, and there is no vortex in the water flow, and the main stream touches the floor. If the water cushion depth is 5cm, water flow turns at the inlet and outlet of the stilling basin, a partial vortex area is formed, the flow velocity in the stilling basin is high, and the main stream touches the bottom. If the basin depth is 10cm, the flow velocity is high at the front end of the stilling basin, and there are only a few vortexes; there are more vortexes occurring at the terminal of the basin; meanwhile the flow velocity is still high, and the main stream touches the bottom. If the basin depth is 15cm, the flow velocity in the front end of the stilling basin is higher than that in the tail end, and the water bodies of energy dissipation is larger compared with the aforesaid three conditions, and there is a water cushion of 1/5 basin depth from the main stream to the basin bottom (the black line in Fig. 15(d) is with the distance of 1/5 basin depth to the bottom plate). If the basin depth is increased to 20cm or 25cm, the water body of dissipation gets larger with wider range vortex, and the flow velocity has been reduced greatly in the front end of the stilling basin, and there is a deep water layer below the main stream, and an obvious submerged hydraulic jump has been occurred.

Based on the flow regime and flow field distribution of the hydraulic jump, when Froude number equals to 9.41, the best depth of shallow-water cushion is 15cm and the corresponding related depth-to-length ratio is 0.125.

2.3 Fr=6.71 (V=2m/s)

(1) Flow regime and flow profile

The occurrence conditions of hydraulic jump in the stilling basin are different at different depths according to the water flow regimes in the stilling basin at six depths (d) of shallow-water cushion which are presented in Fig. 16. In case that the water cushion depth is 0cm (there is no shallow-water cushion), 5cm or 10cm, the water flow regime is similar along downstream the discharge chute and in the shallow-water cushion, and it varies as follows: there is no hydraulic jump, the flow regime bends, and hydraulic jump in far-forth driving form occurs. In case that the basin depth is 15cm, there is intense fluctuation in water in the basin; when compared with the stilling basin with the depth of

Preprints (www.preprints.org) | NOT PEER-REVIEWED | Posted: 23 October 2017 doi:10.20944/preprints201710.0147.v1

15cm corresponding to the aforesaid two Froude numbers, there are more water bodies of energy dissipation in the basin at this Froude number, but the critical hydraulic jump has not been formed entirely. In case that the basin depth is 20cm or 25cm, the stilling basin is occupied by water body, and the submerged type hydraulic jump occurs. Therefore, in terms of flow regime, relatively perfect hydraulic jump occurs in stilling basin when the shallow-water cushion depth of 15cm~20cm (depth-to-length ratio: 0.125~0.167).

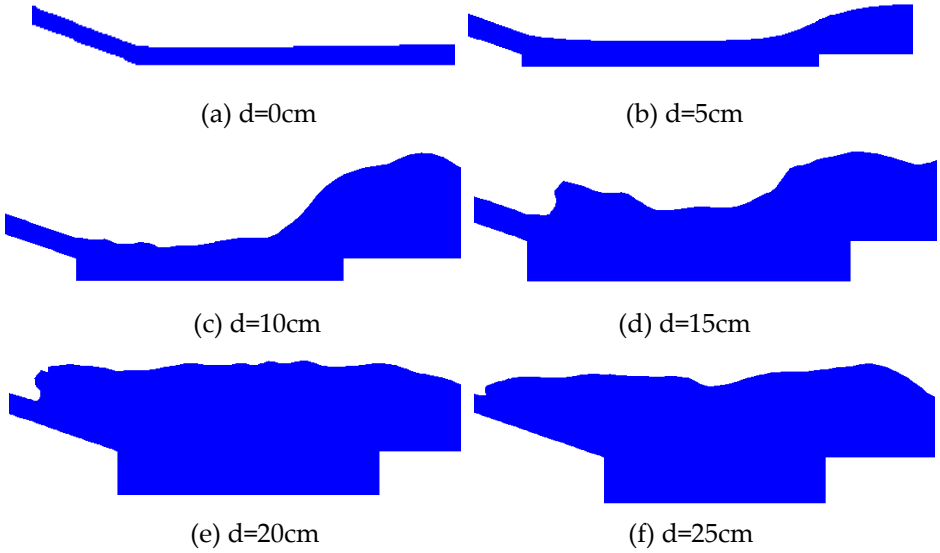

Fig. 16 Schematic diagram for flow regimes under six conditions

From comparison of profiles of free surface in the stilling basin at six depths of shallow-water cushion (Fig. 17), the same observation can be seen that the flow profiles under different conditions vary greatly, and relatively perfect flow profile is obtained when the water cushion depth is 15cm~20cm.

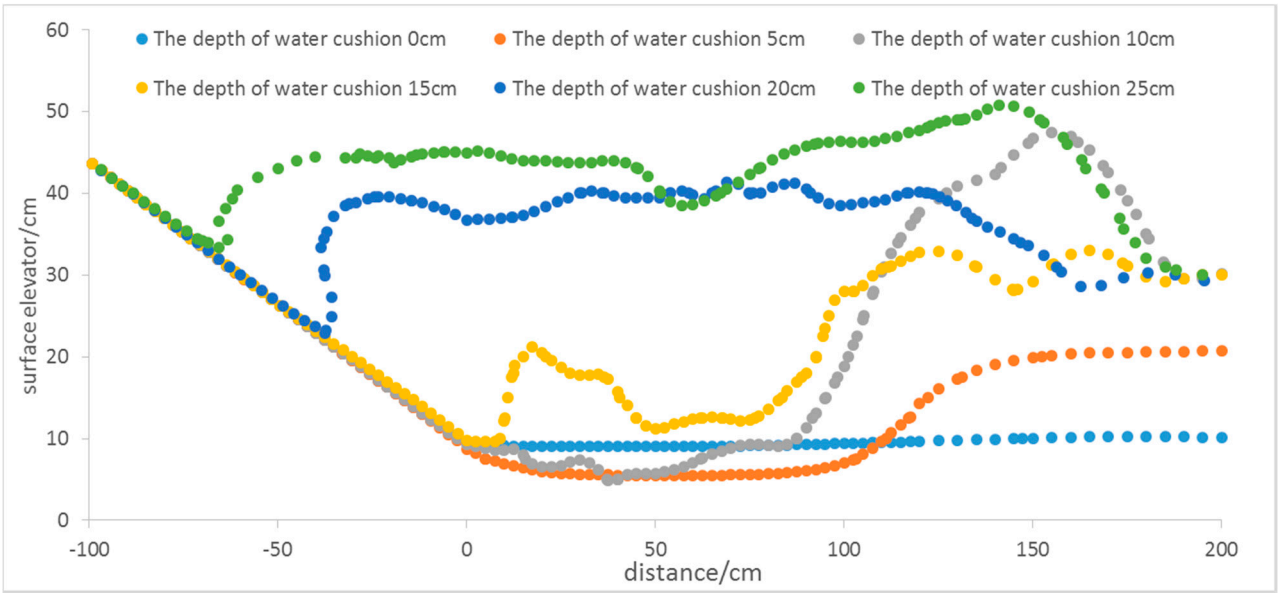

Fig. 17 Comparison of flow profiles at different water cushion depths (Fr=6.71)

(2) Flow field structure

Velocity fields of local flow in the six stilling basins are presented in Fig.18. It shows that under different conditions, the water flow is different at the inlet and the stilling basin section, and the

Preprints (www.preprints.org) | NOT PEER-REVIEWED | Posted: 23 October 2017 doi:10.20944/preprints201710.0147.v1

velocity varies differently in the vertical direction, and the quantity and intensity of the vortex generated in the water flow are different.

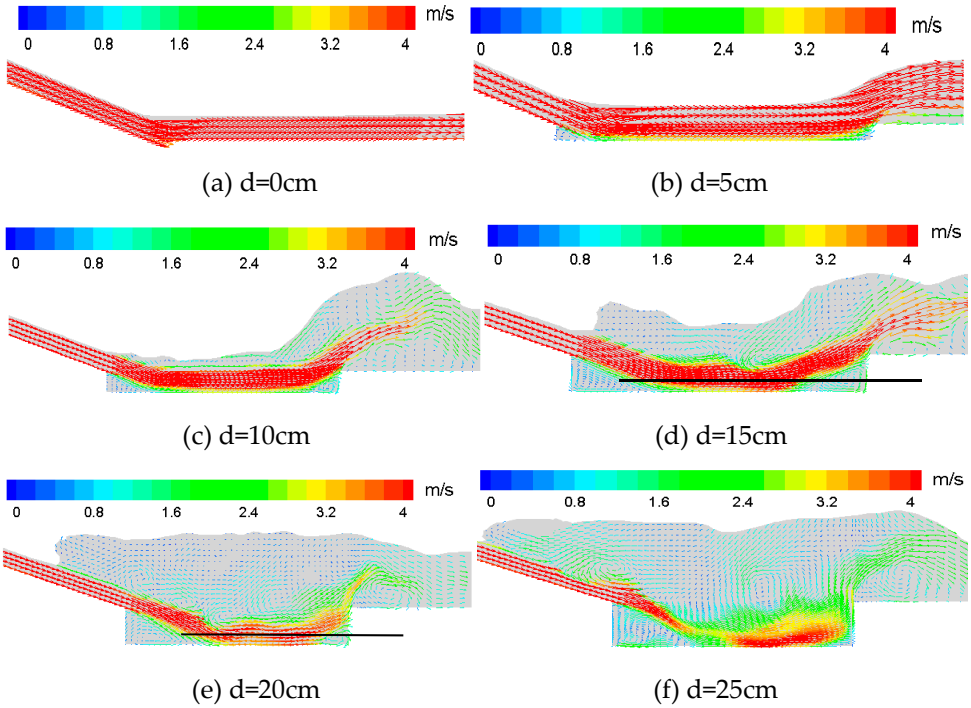

Fig. 18 Velocity vector of local flow in stilling basin

Compared with the six shallow-water cushion depth conditions corresponding to the aforesaid two Froude numbers (Fig. 12 and Fig. 15), the flow velocity vector charts corresponding to six depths shown in Fig. 18 are similar. In case of no shallow-water cushion (0cm), the flow velocity downstream the chute is not reduced obviously, there is no vortex in the water flow, and the main stream touches the floor directly. If the depth of the shallow-water cushion is 5cm, water flow turns at the inlet and outlet of the stilling basin, a partial vortex area is formed, the flow velocity in the stilling basin is high, and the main stream touches the bottom. If the basin depth is 10cm, the flow velocity in the whole stilling basin is high, there are only a few vortexes; at the terminal of the basin, the surface in the horizontal direction increases greatly, and the main stream touches the basin bottom. If the basin depth is 15cm, the flow velocity is not reduced greatly from the front end to terminal of the stilling basin, but there are more water bodies of energy dissipation when compared with the aforesaid three conditions, a water cushion is formed between the main stream and the basin bottom (the black line in Fig. 18(d) is with the distance of 1/5 basin depth to the bottom plate). If the basin depth is increased to 20cm or 25cm, the water body of dissipation gets larger with wider range vortex, and the flow velocity has been reduced greatly in the front end of the stilling basin, and there is a deep water layer below the main stream, and an obvious submerged hydraulic jump has been occurred.

Based on the flow regime and flow field distribution of the hydraulic jump, when Froude number equals to 6.71, the best shallow-water cushion depth is 15~20cm and the corresponding related depth-to-length ratio is 0.125~0.167.

2.4 Fr=4.89 (V=6.5m/s)

(1) Flow regime and flow profile

The occurrence conditions of hydraulic jump in the stilling basin are different at different depths according to the water flow regimes in the stilling basin at six depths (d) of shallow-water cushion which are presented in Fig. 19. In case that the water cushion depth is 0cm (there is no shallow-water cushion), 5cm, 10cm or 15cm, the water flow regime is similar along downstream the discharge chute and in the shallow-water cushion, the water face is flat, and no hydraulic jump occurs. In case that

Preprints (www.preprints.org) | NOT PEER-REVIEWED | Posted: 23 October 2017 doi:10.20944/preprints201710.0147.v1

the basin depth is 20cm, there is intense fluctuation in water in the basin; compared with the aforesaid four water cushion depths, there are more water bodies of energy dissipation in the water cushion, and the critical hydraulic jump occurs. In case that the basin depth is 25cm, the stilling basin is occupied by water body, and the submerged type hydraulic jump occurs. Therefore, in terms of flow regime, relatively perfect hydraulic jump occurs in the stilling basin when the shallow-water cushion depth of 20cm (depth-to-length ratio: 0.167).

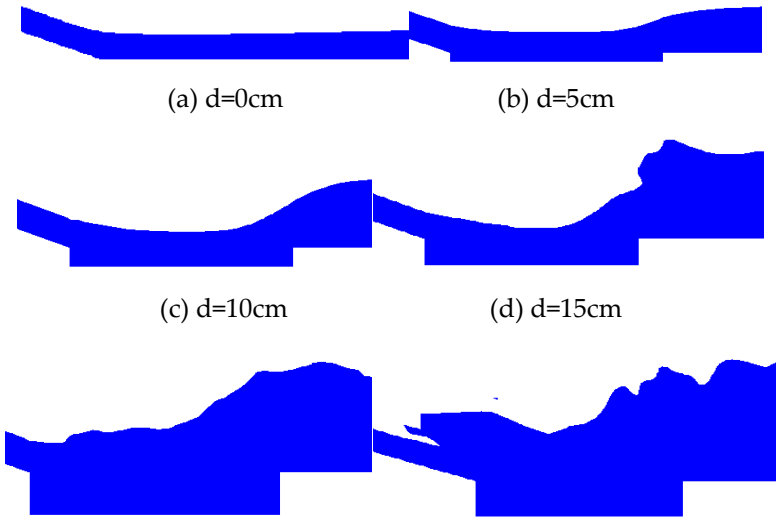

Fig. 19 Schematic diagram for flow regimes under six conditions

From comparison of profiles of free surface in the stilling basin at six depths of shallow-water cushion (Fig. 20), the same observation can be seen that the flow profiles under different conditions vary greatly, and relatively perfect flow profile is obtained when the water cushion depth is 20cm.

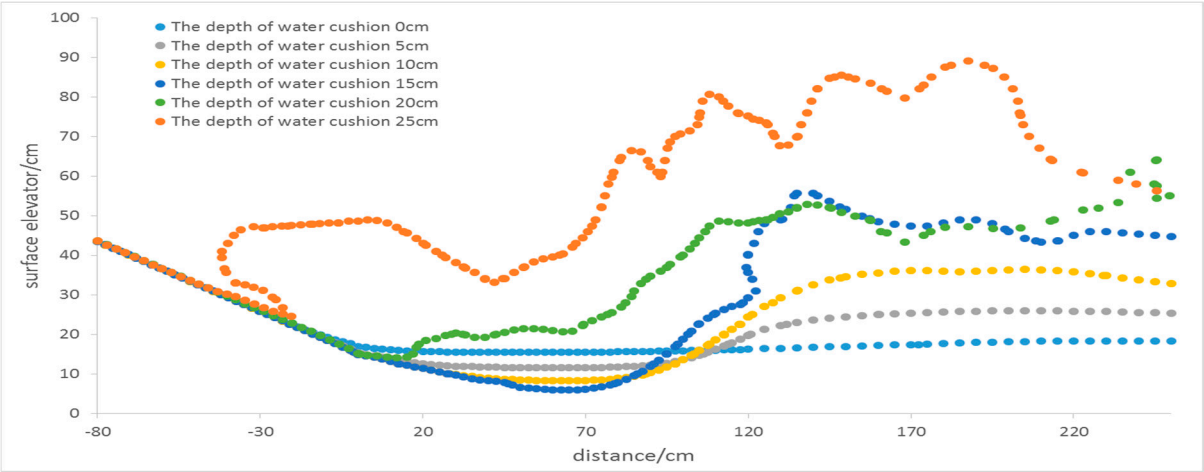

Fig. 20 Comparison of flow profiles at different water cushion depths (Fr=4.89)

(2) Flow field structure

Velocity fields of local flow in the six stilling basins are presented in Fig.21. It shows that under different conditions, the water flow is different at the inlet and the stilling basin section, and the velocity varies differently in the vertical direction, and the quantity and intensity of the vortex generated in the water flow are different.

Preprints (www.preprints.org) | NOT PEER-REVIEWED | Posted: 23 October 2017 doi:10.20944/preprints201710.0147.v1

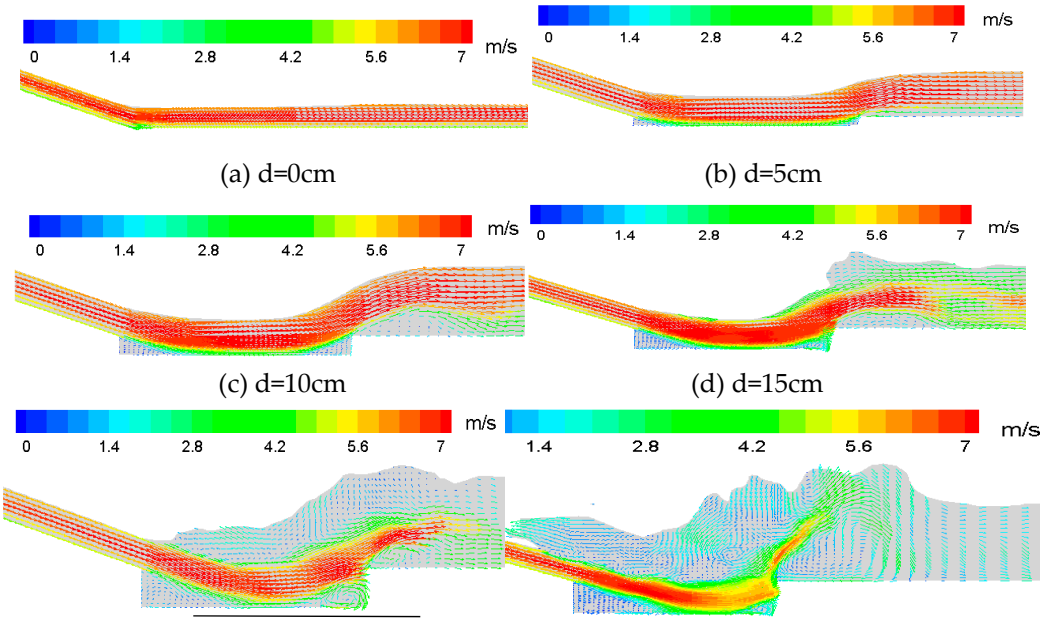

Fig. 21 Velocity vector of local flow in stilling basin

Compared with the operating conditions at the aforesaid Froude numbers, the flow velocity vector charts at the depths of 0cm (there is no shallow-water cushion), 5cm, 10cm and 15cm as shown in Fig. 21 are similar; the flow turns in the stilling basin, there are only a few vortexes, the flow velocity is not reduced, and the main stream impacts the basin bottom inordinately. In case that the basin depth is 20cm, there are more vortexes in the stilling basin, the flow velocity is reduced from the front end to the tail end. In the tail end after the stilling basin terminal, the flow velocity is reduced greatly, and there is a water cushion of 1/5 basin depth from the main stream to the basin bottom is formed (the black line in Fig. 21(e) is with the distance of 1/5 basin depth to the bottom plate). In case that the basin depth is increased to 25cm, the water body of dissipation gets larger with wider range vortex, and the flow velocity has been reduced greatly in the stilling basin, and there is a deep water layer below the main stream, and an obvious submerged hydraulic jump has been occurred.

Based on the flow regime and flow field distribution of the hydraulic jump, when Froude number equals to 4.89, the best depth of shallow-water cushion is 20cm and the corresponding related depth-to-length ratio is 0.167.

2.5 Fr=5.17 (V=8m/s)

(1) Flow regime and flow profile

The occurrence conditions of hydraulic jump in the stilling basin are different at different depths according to the water flow regimes in the stilling basin at six depths (d) of shallow-water cushion which are presented in Fig. 22. In case that the water cushion depth is 0cm (there is no shallow-water cushion), 5cm, 10cm or 15cm, the water flow regime is similar along downstream the discharge chute and in the shallow-water cushion, the water face is flat, and no hydraulic jump occurs. In case that the basin depth is 20cm, there is intense fluctuation in water in the basin; compared with the aforesaid four water cushion depths, there are more water bodies of energy dissipation in the water cushion, but there is no critical hydraulic jump. In case that the basin depth is increased to 25cm, the stilling basin is occupied by a large water body, and submerged type hydraulic jump occurs. Therefore, in terms of flow regime, relatively perfect hydraulic jump occurs in the stilling basin when the shallow-water cushion depth of 20~25cm (depth-to-length ratio: 0.167~0.208).

Preprints (www.preprints.org) | NOT PEER-REVIEWED | Posted: 23 October 2017 doi:10.20944/preprints201710.0147.v1

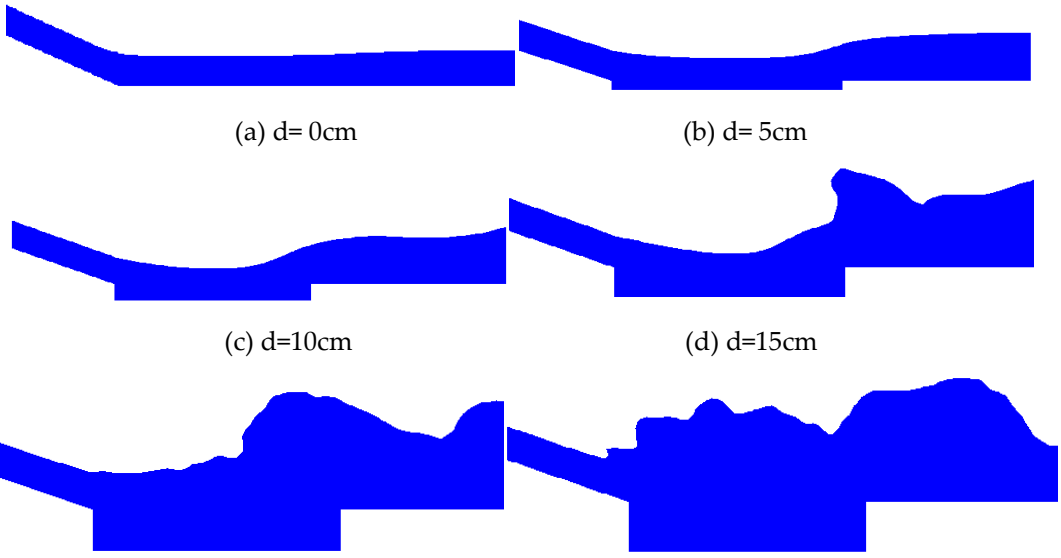

(a) d= 0cm (b) d= 5cm

(c) d=10cm (d) d=15cm

(e) d=20cm (f) d=25cm

Fig. 22 Schematic diagram for flow regimes under six conditions

From comparison of profiles of free surface in the stilling basin at six depths of shallow-water cushion (Fig. 23), the same observation can be seen that the flow profiles under different conditions vary greatly, and relatively perfect flow profile is obtained when the water cushion depth is 20~25cm.

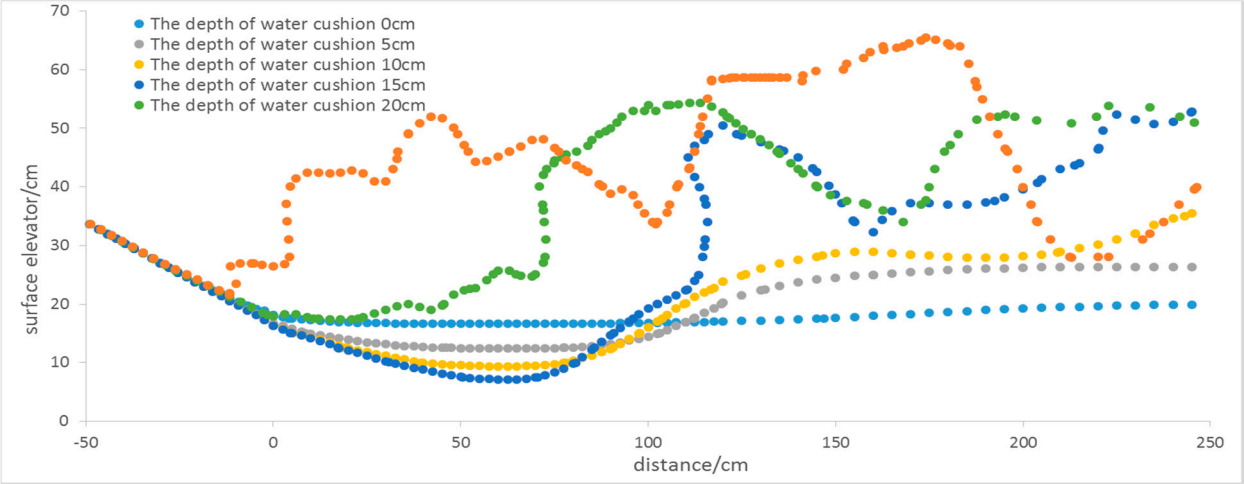

Fig. 23 Comparison of flow profiles at different water cushion depths (Fr=5.17)

(2) Flow field structure

Velocity fields of local flow in the six stilling basins are presented in Fig.24. It shows that under different conditions, the water flow is different at the inlet and the stilling basin section, and the velocity varies differently in the vertical direction, and the quantity and intensity of the vortex generated in the water flow are different.

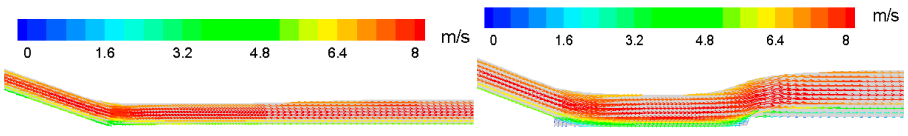

(a) d=0cm (b) d=5cm

Preprints (www.preprints.org) | NOT PEER-REVIEWED | Posted: 23 October 2017 doi:10.20944/preprints201710.0147.v1

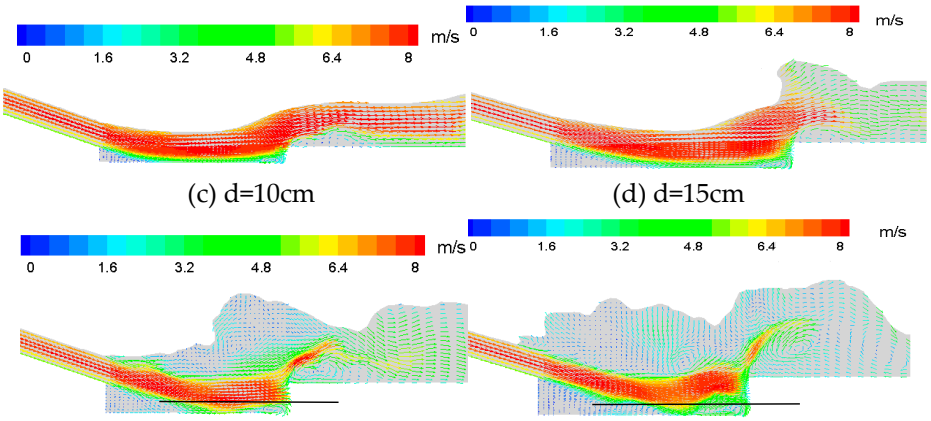

Fig. 24 Velocity vector of local flow in stilling basin

Compared with the operating conditions at the aforesaid Froude numbers, the flow velocity vector charts at the depths of 0cm (there is no water cushion), 5cm, 10cm and 15cm as shown in Fig. 24 are similar; the flow turns in the stilling basin, there are only a few vortexes, the flow velocity is not reduced, and the main stream touches the basin bottom inordinately. In case that the basin depth is 20cm, there are more vortexes in the stilling basin, but no critical hydraulic jump occurs, the main stream impacts the tail ridge of the stilling basin directly, and a water cushion of 1/5 basin depth from the main stream to the basin bottom is formed (the black line in Fig. 24(e) is with the distance of 1/5 basin depth to the bottom plate). In case that the basin depth is 25cm, the water body of dissipation gets larger with wider range vortex, and the flow velocity has been reduced greatly in the stilling basin, and an obvious submerged hydraulic jump has been occurred, and a water cushion of greater than 1/5 basin depth from the main stream to the basin bottom is formed (the black line in Fig. 24(f) is with the distance of 1/5 basin depth to the bottom plate).

Based on the flow regime and flow field distribution of the hydraulic jump, when Froude number equals to 5.17, the best shallow-water cushion depth is 20~25cm and the corresponding related depth-to-length ratio is 0.167~0.208.

3 Conclusion

For the first time the best water cushion depth is defined based on the flow regime of hydraulic jump and underflow speed in this paper at the beginning; namely, in case of critical hydraulic jump in the basin, the best water cushion depth is located where the minimum distance to the bottom of the stilling basin is 1/5~1/4 of the water cushion depth. Then the theoretical analysis is conducted to obtain the varying pattern between the Froude number (Fr) at inlet of the stilling basin with shallow-water cushion and the flow velocity at discharge chute inlet (V) under different ratios between different inclinations of discharge chute (θ) and depth ratios of inlet (m); namely, instead of monotonic change, Fr firstly reduces and then increases as V increases, and the parameters of inflection point (critical flow velocity and critical Fr) increase as the inclinations of discharge chute (θ) and depth ratios of inlet (m) increase. After the reliability of the large eddy simulation calculation results are verified by a model test, 30 computing cases are selected including five different Froude numbers and six shallow-water cushion depths based on the theoretical analysis results, for calculating the hydraulic factors such as flow profile, flow regime and flow velocity in the stilling basin with shallow-water cushion; and the varying pattern between the best depth of stilling basin with shallow-water cushion (depth-length ratio) and the inflow Froude number as follows is obtained. It shows that before reaching the critical Froude number, the best depth of stilling basin with shallow-water cushion varies little as the change of the Froude number, however after the critical Froude number is reached, the best depth-length ratio of stilling basin with shallow-water cushion increases as the Froude number increases. In terms of this study (m=36.3, θ=17°), the best depth-to-length ratio of the shallow-water cushion related to the selected Froude numbers is 1/8~1/5

basically. But it is noticeable that, at the different m and discharge chute inclination (θ), the best depth-to-length ratio of the shallow-water cushion may be different too, which can be studied accordingly as per the study method in this paper.

Acknowledgments: This research work was supported by the National Key Research Development Plan (No. 2016YFC0401705), National Natural Science Foundation of China (No.51209154), (No.51079091).

Author Contributions: Qiulin Li carried out the model simulations and result analysis as well as writing of the manuscript. Lianxia Li provided the prototype field data and relevant engineering documents. Huasheng Liao took the leadership of whole project and participated in the discussion and decision-making process. Jingjing Wei developed and tested the numerical code. Shengyin Jiang and Faxing Zhang contributed to the drafting of manuscript and responses to the referees. All the authors participated and contributed to the final manuscript.

Conflicts of Interest: The authors declare no conflict of interest

Reference

[1] Chanson H. Current knowledge in hydraulic jumps and related phenomena. A survey of experimental results[J]. European Journal of Mechanics / B Fluids, 2009, 28(2):191-210.

[2] H. Chanson. Hydraulic condition for undular-jump formations [J]. Journal of Hydraulic Research, 2001, 39(2):203-209.

[3] Alikhani A, Behrozi-Rad R, Fathi-Moghadam M. Hydraulic jump in stilling basin with vertical end sill [J]. International Journal of Physical Sciences, 2010, 5(1):25-29.

[4] Zare H K, Doering J C. Forced Hydraulic Jumps below Abrupt Expansions [J]. Journal of Hydraulic Engineering, 2011, 137(8):825-835.

[5] Champagne T M, Barlock R R, Ghimire S R, et al. Scour Reduction by Air Injection Downstream of Stilling Basins: Optimal Configuration Determination by Experimentation[J]. Journal of Irrigation & Drainage Engineering, 2016, 142(12):04016067.

[6]LI Tianxiang. Investigation on Hydraulic Performances of Stilling Basin with Shallow-water Cushion [D].Chendu: State Key Laboratory of Hydraulics and Mountain River R & D in Sichuan University,2006.

[7]SU Peilan, LIAO Huasheng, LI Tianxiang, et al. Experimental Investigation on Hydraulic Properties in Stilling Basin with Shallow-water Cushion(SBSC)[J].Journal of Sichuan University: Engineering Science Edition, 2009,02:35-41.

[8]RU Yongshen, LIAO Huasheng, LI Lianxiao, et al. Numerical Simulation and Experimental investigation on Stilling Basin with Shallow-water Cushion[J].Journal of Hydroelectric Engineering, 2010,02:36-41+126.

[9]LIU Da, LIAO Huasheng, LI Lianxia, et al. Large Eddy Simulation on Stilling Basin with Shallow-water Cushion[J]. Journal of Sichuan University: Engineering Science Edition,2014, 05:28-34.

[10]LI Lianxia, LIAO Huasheng, LIU Dewei, et al. Influence of Inlet form on Hydraulic Jump in Stilling Basin with Shallow Water Cushion[J]. Journal of Hydroelectric Engineering,2015, 05:57-65.

[11]LI Lianxia, LIAO Huasheng, LIU Da, et al. Experimental investigation of the optimization of stilling basin with shallow water cushion used for low Froude number energy dissipation[J]. Journal of Hydrodynamics B series, 2015，27(4):522-529.

[12] LIU Da, LIAO Huasheng, LI Lianxia, et al. Effects of Inflow Angle to the Flow Characteristics in Stilling Basin with Shallow-water Cushion[J].Water Power,2016,04:49-52.

[13] JIANG Shenyin. Experimental Study on the Model of Double Shallow Water Cushion [J].Shanxi Shuili,2011,02:67-68.

[14] LIU Da, LI Lianxia, HUANG Bensheng, et al. Numerical Simulation and Experimental Investigation on Stilling Basin with Double Shallow-water Cushions [J]. Journal of Hydraulic Engineering,2012,05:623-630.

[15]WAN Jiwei, NIU Zhengming, LI Lu, et al. Experimental Study of Hydraulic Characteristics of Small-trajectory Angle Drop Sill Combined with Stilling Basin with Shallow-water Cushion [J].Journal of Hohai University(Natural Sciences) ,2012,03:300-306.

[16]SUN Shuangke, LIU Haitao, XIA Qingfu, et al. Study on Stilling Basin with Step-down Floor for Energy Dissipation of Hydraulic Jump in High Dams[J]. Journal of Hydraulic Engineering,2005,(10):1188-1193.

[17]YANG Yongsen, YANG Yongquan, SHUAI Qinghong. The Hydraulic and Aeration Characteristics of Low Froude Number Flow over a Step Aerator[J]. Journal of Hydraulic Engineering,2000,(02):27-31.

[18] Riazi R, Bejestan M S, Kashkouli H, et al. Effect of roughness on characteristics of bed B-jump in stilling basin with abrupt drop[J]. Research on Crops, 2012, 13(3):1137-1141.

[19] N. Eroğlu, N. Tokyay. Statistical approach to geometric properties of wave-type flow occurring at an abrupt drop[J]. 2012, 27(4):911-919.

[20] Sabzkoohi A M, Kashefipour S M, Bina M. Investigation of effective parameters on stepped and straight drops energy dissipation using physical modeling [J]. Journal of Food Agriculture & Environment, 2011, 9(3):748-753.

[21] Michele Mossa PhD MIAHR, Antonio Petrillo. Tailwater level effects on flow conditions at an abrupt drop[J]. Journal of Hydraulic Research, 2003, 41(1):39-51.

[22] Hager W H, Kawagoshi N. Hydraulic jumps at rounded drop [J]. Proceedings of the Institution of Civil Engineers Part Research & Theory, 1990, 89(4):443-470.

[23] Rice C E, Kadavy K C. Riprap design upstream of straight drop spillways [J]. Transactions of the Asae, 1992, 34(4):1715-1725.

[24] Ram K V S, Prasad R. Spatial B-Jump at Sudden Channel Enlargements with Abrupt Drop[J]. Journal of Hydraulic Engineering, 1998, 124(6):643-646.

[25]Smagorinsky J S. Smagorinsky, J.: General Circulation Experiments with the Primitive Equations. Monthly Weather Review 91, 99-165[J]. Monthly Weather Review, 1963, 91(3):99-164.

[26] Deardorff J W. A numerical study of three-dimensional turbulent channel flow at large Reynolds numbers[J]. Journal of Fluid Mechanics, 2013, 41(2):453-480.

[27] Moin P, Kim J. Numerical investigation of turbulent channel flow [J]. Journal of Fluid Mechanics, 2006, 118(-1):1280-4.

[28] Song C C S. A weakly compressible flow model and rapid convergence methods [J]. Journal of Fluids Engineering, 1988, 110(4):441-445.

[29] Michele Mossa PhD MIAHR, Antonio Petrillo. Tail-water level effects on flow conditions at an abrupt drop [J]. Journal of Hydraulic Research, 2003, 41(1):39-51.